NONLINEAR DYNAMICS OF A PIEZOELECTRICALLY- ACTUATED MICROCANTILEVER SENSOR

S.Nima Mahmoodi
Department of Mechanical Engineering,
Clemson University,
Clemson, SC 29634-0921 USA
seyedm@clemson.edu

Nader Jalili
Department of Mechanical Engineering,
Clemson University,
Clemson, SC 29634-0921 USA
jalili@clemson.edu

Mohammed F. Daqaq
Department of Mechanical Engineering,
Clemson University,
Clemson, SC 29634-0921 USA
mdaqaq@clemson.edu

Abstract

NanoMechanical Cantilever Sensors (NMCS) have recently emerged as an effective means for label-free chemical and biological species detection. They operate through the adsorption of species on the functionalized surface of cantilevers. Through this functionalization, molecular recognition is directly transduced into a micromechanical response. In order to effectively utilize these sensors in practice, the chief technical issue related to modeling must be addressed in order to correctly relate the micromechanical response to the adsorbed species. Along this line of reasoning, this paper presents a general nonlinear-comprehensive modeling framework for piezoelectrically-actuated microcantilevers and validate it both analytically and experimentally. The proposed model considers both longitudinal and flexural vibrations of the microcantilever sensor and their coupling in addition to the ever-present nonlinearities due to geometry of the microcantilever. More specifically, it is demonstrated that the electromechanical coupling in these sensors is also nonlinear which appears in quadratic form. Through extensive experimental measurements, the coefficient of such quadratic nonlinear term is determined which compares well with both analytical and numerical results. Taking into account the inextensibility feature of such sensors, the coupled longitudinal and flexural equations of motion are reduced to one nonlinear flexural equation. The resultant nonlinear equation of motion is then solved using the method of Multiple Scales to arrive at the frequency response of the system, analytically. Consequently, the system response to a number of periodic excitations with different amplitudes is experimentally and analytically investigated which matches the analytical results very well. Finally, the frequency response results clearly demonstrate the presence of nonlinear quadratic term in electromechanical coupling in these sensors. This is a critical observation when designing and employing such sensors for practical applications.

Keywords

Piezoelectrically-actuated microcantilevers, Electro-mechanical coupling, Nonlinear flexural vibration of the microcantilever.

1. Introduction

NanoMechanical Cantilever Sensors (NMCS) have recently emerged as an effective means for label-free chemical and biological species detection. Selectivity, low cost, and easy mass production make them an enabling technology for micro- and nano-detection techniques. NMCS operate through the adsorption of species on the functionalized surface of cantilevers. Through this functionalization, molecular recognition is directly transduced into a micromechanical response. More specifically, piezoelectrically-actuated NMCS have been recently employed to improve the MEMS devices for better actuation and sensing quality. For this purpose and considering small scale nature of these microcantilevers, a nonlinear-comprehensive modeling development is needed.

This research is motivated by many applications of such microcantilevers including, but not limited to, microsensors/actuators, energy harvesting and scanning force microscopy. The dynamic modeling of a piezoelectric transducer, based on nonlinear piezoelectric mechanical properties, has been investigated to describe the harmonic generation that occurs on velocity signal analysis when transducer is driven at high voltage [1]. The vibration produced by piezoelectrically-actuated beam can drive small electrical motors. In this system, piezoelectric transforms electrical energy into mechanical vibration that is transformed via frictional contact between tip and slider to motion of the driven part [2]. A broad range of piezoelectrically-actuated microcantilever has been utilized in Scanning Force Microscopy (SFM). Atomic force microscopy (AFM) [3], friction force microscopy (FFM) [4] and biological mass and sequencing measurements [5] serve as demonstrable examples of such applications.

Mechanical properties of the piezoelectric layer should be deeply investigated with proper electromechanical properties applied to the mathematical model. Piezoelectric beams for application in sensors and actuators have been studied and a comparative study demonstrates that the piezoelectric effect is much higher than electrostatic activation in many applications [6]. Nonlinear behavior of piezoelectric ceramics has also been researched and its characterization under high excitations has been studied [7]. A method to measure the mechanical nonlinear coefficients of piezoceramics with high signal excitation has been developed [8, 9]. The bending of layered piezoelectric beams subjected to electrical and mechanical loadings has been researched and effect of strain on electrical field in the layer has been obtained [10]. A variational energy approach has been utilized to analyze electromechanical coupling of piezoelectric beams [11]. Coupled electromechanical response of an infinitely long piezoelectric tube as a sensor/actuator has been investigated by variational approach [12].

Nonlinearity in equations of motion and frequency response is obtained from nonlinear geometry of the beam vibration and inextensibility of the beam. Using a geometrical approach, the equations of motion for nonlinear flexural-flexural-torsional vibrations of inextensible beams have been obtained and the stability of the systems has been investigated [13, 14]. Piezoelectrically-actuated cantilevers considering linear electromechanical stress-strain relations have also been investigated [15, 16] and the equations of motion of the systems have been derived. In addition, equations of motion of piezoelectrically-driven microcantilever with nonlinear geometry have been derived and nonlinear cubic and quadratic terms due to the presence of piezoelectric layer on the microcantilever have been explored [17-19].

This paper presents a general nonlinear-comprehensive modeling framework for piezoelectrically-actuated microcantilevers and validate it both analytically and experimentally. The proposed model considers both longitudinal and flexural vibrations of the microcantilever sensor and their coupling in addition to the ever-present nonlinearities due to geometry of the microcantilever. More specifically, it is demonstrated that the electromechanical coupling in these sensors is also nonlinear which appears in quadratic form. Through extensive experimental measurements, the coefficient of such quadratic nonlinear term is determined which compares well with both analytical and numerical results.

2. Governing Equations of Motion

In this section, the governing equations of motion for the flexural vibrations of a piezoelectrically-actuated microcantilever sensor are derived following the pattern found in Crespo da Silva [13]. As shown in Fig. 1a, the piezoelectric layer is deposited on the top side of the microcantilever and is utilized to actuate the beam by supplying a voltage, *P(t)*. The dynamics of the beam are described by a longitudinal displacement *u(s,t)* and a transversal displacement *v(s,t)*, Fig. 1b, where *s* denotes the arclength and *t* denotes the time. To describe the beam dynamics, two coordinate systems are utilized: the (*x*, *y, z*) system is considered to be inertial, while the (ξ, θ, ζ) system is a local principal system. The relationship between the principal and the inertial coordinates is described by the Euler rotation, $\psi(s,t)$. For an element of length *ds*, ψ can be written as, Fig. 1b

$$\psi = \tan^{-1}\frac{v'}{1+u'}, \tag{1}$$

where the over prime denotes derivative with respect to the arclength *s*. To derive the strain-displacement relations, the Euler-Bernoulli beam theory is adapted which involves the assumptions that the angular deformation due to shear is negligible when compared to the flexural deformations due to bending and that the rotation of a differential element is very small in relation to its translation. By examining Fig. 1b, it becomes evident that, before deformation, the position vector of an arbitrary point on the neutral axis of the beam is given by $\vec{r}_0 = s\,\mathbf{e}_x$. After deformation, its position becomes $\vec{r} = (s+u)\mathbf{e}_\xi + v\mathbf{e}_\theta$. Using these position vectors, the strain along the neutral axis of a differential element *ds* can be expressed as

$$\varepsilon_0 = \left(\frac{\partial\vec{r}}{\partial s}.\frac{\partial\vec{r}}{\partial s}\right)^{\frac{1}{2}} - \left(\frac{\partial\vec{r}_0}{\partial s}.\frac{\partial\vec{r}_0}{\partial s}\right)^{\frac{1}{2}} = \sqrt{\left(1+u'\right)^2 + v'^2} - 1. \tag{2}$$

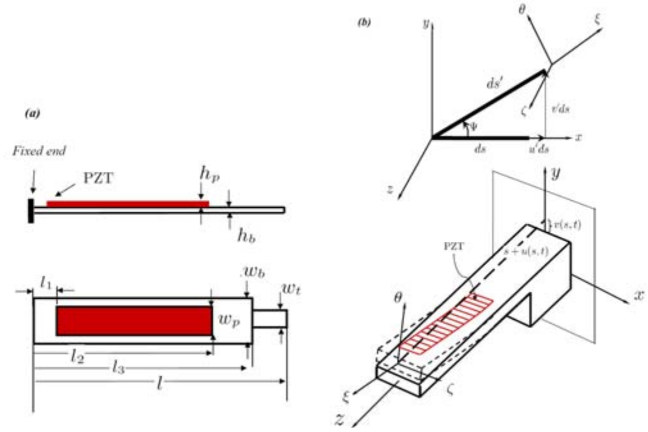

Figure 1. a) Schematic of the microcantilever sensor and, b) The principal and inertial coordinate systems.

and the axial strain at a point having the coordinates (ξ,θ,ζ) can be written as

$$\varepsilon_{11} = \varepsilon_0 - \theta\rho_\zeta. \tag{3}$$

where ρ_ζ is the beam curvature given by $\rho_\zeta = v'' - v''u' - v'u'' - v''v'^2$. Further details on the derivation of equation (3) can be found in [18, 19]. Next, using the constitutive equations, we relate the axial stress developed in a differential element to its axial strain. For silicon, the constitutive equations can be written as

$$\sigma_{11}^b = E_b\varepsilon_{11}^b \tag{4}$$

where $E_b = \dfrac{E_b^*}{(1-\nu_b^2)}$. Here, E_b^* is modulus of elasticity for silicon and ν_b is its Poisson's ratio. Further, for the piezoelectric material the constitutive equations are given by [11]

$$\sigma_{11}^p = E_p\varepsilon_{11}^p + \frac{\alpha_1}{2}\left(\varepsilon_{11}^p\right)^2 - E_p d_{31}\frac{P(t)}{h_p}, \tag{5}$$

Now, the total strain energy of the beam and piezoelectric layer can be written as

$$\begin{aligned} U &= \frac{1}{2}\int_0^{l1}\iint_A\left(\sigma_{11}^b\varepsilon_{11}^b\right)dA\,ds + \frac{1}{2}\int_{l1}^{l2}\iint_A\left(\sigma_{11}^b\varepsilon_{11}^b\right)dA\,ds \\ &+\frac{1}{2}\int_{l1}^{l2}\iint_A\left(\sigma_{11}^p\varepsilon_{11}^p\right)dA\,ds \\ &+\frac{1}{2}\int_{l2}^{l3}\iint_A\left(\sigma_{11}^b\varepsilon_{11}^b\right)dA\,ds + \frac{1}{2}\int_{l3}^{l}\iint_A\left(\sigma_{11}^b\varepsilon_{11}^b\right)dA\,ds \\ &+\frac{1}{2}\int_0^{l} EA(s)\left(u'^2 + u'v'^2 + \frac{1}{4}v'^4\right)ds \end{aligned} \tag{6}$$

where dA is the cross sectional area of a differential beam element and

$$\begin{aligned} EA(s) &= \left(H_0 - H_{l3}\right)E_b w_b h_b + \left(H_{l1} - H_{l2}\right)E_p w_p h_p \\ &+\left(H_{l3} - H_l\right)E_b w_t h_b \end{aligned} \tag{7}$$

where $H(s)$ is the Heaviside function, w denotes the width, h denotes the thickness, and the subscripts b, p, and t indicate the silicon, piezoelectric material, and the beam tip, respectively, Fig. 1 a. It is worth noting that the potential energy of the electric field has not been included in the total potential of the system. This stems from the fact that, we only consider the direct piezoelectric effect in which the voltage $P(t)$ is prescribed and not considered as a degree of freedom.

Next, the kinetic energy of the system can be expressed as

$$T = \frac{1}{2}\int_0^{l} m(s)(\dot{u}^2 + \dot{v}^2)\,ds\ , \tag{8}$$

where

$$m(s) = \left(\rho_b + \left(H_{l1} - H_{l2}\right)\rho_p\right), \tag{9}$$

and ρ_b and ρ_p are the linear mass densities of silicon and the piezoelectric layer, respectively.

Using equations (6)-(8), the Lagrangian of the system, $L = T - U$ can be written as

$$\begin{aligned} L &= \frac{1}{2}\int_0^{l}\Big\{m(s)(\dot{u}^2+\dot{v}^2) - K(s)\left(v''^2 - 2v''^2 v'^2 - 2v''^2 u'\right. \\ &\left.-2v'v''u''\right) + K_p(s)\left(v'' - v''u' - v'u'' - v''v'^2\right)P(t) \\ &-\frac{\alpha_1}{2}I_{np}(s)v''^3 - EA(s)\left(u'^2 + u'v'^2 + \frac{1}{4}v'^4\right)\Big\}ds, \end{aligned} \tag{10}$$

where

$$\begin{cases} K(s) = \left(H_0 - H_{l1}\right)E_b I_b + \left(H_{l1} - H_{l2}\right)E_b\left(I_b + w_b h_b y_n^2\right) \\ +\left(H_{l1} - H_{l2}\right)E_p I_p + \left(H_{l2} - H_{l3}\right)E_b I_b + \left(H_{l3} - H_l\right)E_b I_t \\ K_p(s) = \left(H_{l1} - H_{l2}\right)\dfrac{w_p}{2}E_p d_{31}\left[\left(h_p + h_b\right) - 2y_n\right] \end{cases} \tag{11}$$

where y_n represents the neutral axis of the beam and is given by

$$y_n = \frac{E_p h_p\left(h_p + h_b\right)}{2\left(E_p h_p + E_b h_b\right)}\quad l_1 < s < l_2 \ \text{ and } y_n = 0 \text{ elsewhere} \tag{12}$$

In addition,

$$\begin{cases} I_b = \dfrac{w_b h_b^3}{12};\ I_t = \dfrac{w_t h_t^3}{12} \\ I_{np}(s) = \left(H_{l1} - H_{l2}\right)\dfrac{w_p}{4}\left[\left(\dfrac{h_b}{2} + h_p - y_n\right)^4 - \left(\dfrac{h_b}{2} - y_n\right)^4\right] \\ I_p = w_p\left(h_p y_n^2 + \left(h_p^2 + h_b h_p\right)y_n + \dfrac{1}{3}\left(h_p^3 + \dfrac{3}{2}h_b h_p^2 + \dfrac{3}{4}h_b^2 h_p\right)\right) \end{cases} \tag{13}$$

Next, we consider that the beam is inextensible, meaning that the neutral axis does not undergo any relative elongations, thereby the strain along the neutral axis is equal to zero and equation (2) reduces to [17]

$$\left(1 + u'\right)^2 + v'^2 = 1\,. \tag{14}$$

Equation (14) is known as the extensibility condition and is used to relate the flexural and the longitudinal vibrations of the beam. To obtain the equations of motion for the flexural vibrations of the sensor, we utilized Hamilton's principle which states that $\int_{t_1}^{t_2}\left(\delta L + \delta W\right)dt = 0$, where δ is the first variation of the functions symbol and W is the work of external forces which is zero in our case. It follows form equation (9), (14), and Hamilton's principle that the equations of motion and the associated boundary conditions can be written as

$$\begin{aligned} &m(s)\ddot{v} + \left(K(s)v''\right)'' + \left(\frac{3\alpha_1}{2}I_{np}(s)v''^2\right)'' + \left[v'\left(K(s)v'v''\right)'\right]' \\ &+\left[v'\int_l^s m(s)\int_0^s\left(\ddot{v}'v' + \dot{v}'^2\right)ds\,ds\right]' - \left[\frac{1}{2}v'\left[K_p(s)v'P(t)\right]'\right]' \\ &+\left[\frac{1}{4}K_p(s)v'^2P(t)\right]'' = \left[\frac{1}{2}K_p(s)P(t)\right]'' \end{aligned} \tag{15}$$

$$v = v' = 0 \quad \text{at } s{=}0; \qquad v'' = v''' = 0 \quad \text{at } s{=}l\,. \tag{16}$$

By examining equation (15), two types of nonlinearities are observed: first the quadratic nonlinearities which are manifested in the third term and is resulting from the material nonlinearities of the piezoelectric layer; second the cubic nonlinearities which are due to the geometry of the beam and appear as nonlinear inertia and stiffness terms (fourth and fifth terms in equation (15)). In addition, the sixth term in equation (15) represents a nonlinear parametric excitation term emanating from the nature of the piezoelectric excitation.

3. Model Discretization

We derive a reduced-order model Equation (15) by utilizing a separation of variables in which the deflection $v(s,t)$ is discretized into

$$v(s,t) = \Phi(s)Q(t)\,, \tag{17}$$

where the $Q(t)$ are the generalized temporal coordinates and the $\Phi(s)$ are chosen as the orthogonal set of basis functions representing the mode shapes of a cantilever beam and given by [20]

$$\phi_n(s) = \cosh(z_n s) - \cos(z_n s) + [\sin(z_n s) - \sinh(z_n s)]\frac{\cosh(z_n) + \cos(z_n)}{\sin(z_n) + \sinh(z_n)}, \quad (18)$$

where the z_n are roots of the following characteristic equation:

$$1 + \cos(z_n)\cosh(z_n) = 0 \quad (19)$$

Substituting equation (18) into equation (15), multiplying the result by the mode shapes, ϕ_n, integrating the outcome over the length of the beam and using the orthonormality properties of the linear mode shapes, we obtain the following set of ordinary-differential equations:

$$\begin{aligned} &\ddot{q}_n(t) + \hat{\mu}_n\dot{q}_n(t) + \omega_n^2 q_n(t) + \hat{g}_{n1}q_n^2(t)P(t) + \hat{g}_{n2}q_n^3(t) \\ &+\hat{g}_{n3}\left(q_n^2(t)\ddot{q}_n(t) + q_n(t)\dot{q}_n^2(t)\right) + \hat{g}_{n5}q_n^2(t) = \hat{g}_{n4}P(t) \end{aligned} \quad (20)$$

where the $\hat{g}_{ni}$ are modal time-independent coefficients defined as

$$\omega_n^2 = \int_0^l \phi_n(s)\left(K(s)\phi_n''(s)\right)'' ds \quad (21a)$$

$$\hat{g}_{n1} = \frac{1}{4}\int_0^l \phi_n(s)\left(K_p(s)\phi_n'^2(s)\right)'' ds - \frac{1}{2}\int_0^l \phi_n(s)\left[\phi_n'\left(K_p(s)\phi_n'(s)\right)'\right]' ds \quad (21b)$$

$$\hat{g}_{n2} = \int_0^l \phi_n(s)\left[\phi_n'(s)\left(K(s)\phi_n'(s)\phi_n''(s)\right)'\right]' ds \quad (21c)$$

$$\hat{g}_{n3} = \int_0^l \phi_n(s)\left[\phi_n'(s)\int_l^s m(s)\int_0^s 2\phi_n'^2(s)ds ds\right]' ds \quad (21d)$$

$$\hat{g}_{n4} = \frac{1}{2}\int_0^l \phi_n(s)K_p''(s)ds \quad (21f)$$

$$\hat{g}_{n5} = \frac{3}{2}\alpha_1\int_0^l \phi_n(s)\left(I_{np}(s)\phi''^2\right)''(s)ds \quad (21g)$$

and $\hat{\mu}_n$ are modal damping coefficients introduced to represent linear damping effects.

4. Primary Resonance of Microcantilever

A microcantilever sensor operates by piezoelectrically exciting the beam at one of its resonance frequencies and observing variations in its dynamic behavior. As such, the primary resonance of the microcantilever must be investigated. Towards that objective, we utilize the method of multiple scales [21] and seek a uniform second-order nonlinear approximate solution of Equation (20) near ω_n. we seek a solution of the form

$$q_n(t;\varepsilon) = q_{0n}(T_0,T_1,T_2) + \varepsilon q_{1n}(T_0,T_1,T_2) + \cdots, \quad (22)$$

We scale the quadratic nonlinearity to appear at the second order of the perturbation problem and scale the damping to balance the effects of forcing and cubic nonlinearities at the third order of the perturbation problem. In other words, we let

$$\hat{\mu} = \varepsilon^2\hat{\mu};\ \hat{g}_{n5} = \varepsilon g_{n5};\ \hat{g}_{ni} = \varepsilon^2 g_{ni} \quad i = 1,2,3,4. \quad (23)$$

Now, substituting equations (22-23) into equation (20) and equating coefficients of like powers of ε yields

$$\left(\varepsilon^0\right): D_0^2 q_{0n} + \omega_n^2 q_{0n} = 0 \quad (24)$$

$$\left(\varepsilon^1\right): D_0^2 q_{1n} + \omega_n^2 q_{1n} = -2D_0D_1q_{0n} - g_{n5}q_{0n}^2 \quad (25)$$

$$\begin{aligned} \left(\varepsilon^2\right): D_0^2 q_{2n} + \omega_n^2 q_{2n} &= -\hat{\mu}_n D_0 q_{0n} - 2D_0D_2q_{0n} - 2D_0D_1q_{1n} \\ &- D_1^2 q_{0n} - 2g_{n5}q_{0n}q_{1n} - g_{n1}q_{0n}^2P(t) - g_{n2}q_{0n}^3 \\ &- g_{n3}\left[\left(D_0^2q_{0n}\right)q_{0n}^2 + q_{0n}\left(D_0q_{0n}\right)^2\right] + g_{n4}P(t) \end{aligned} \quad (26)$$

The solution of the first-order problem, equation (24), can be expressed as

$$q_{0n} = A_n(T_1,T_2)e^{i\omega_nT_0} + cc, \quad (27)$$

where A_n is a complex valued function that will be determined at a later stage in the analysis and cc is the complex conjugate of the preceding term. Substituting equation (27) into equation (25), and eliminate any secular terms, and obtain $D_1A_n = 0$. Therefore, A_n must be independent of T_1. Considering this fact, and substituting the solution of equation (25) into (26), it can be written as

$$\begin{aligned} D_0^2q_{2n} + \omega_n^2q_{2n} &= -\left[\hat{\mu}i\omega_nA_n + 2i\omega_nD_2A_n\right]e^{i\omega_nT_0} \\ &-\left(3g_{n2} - \frac{10}{3}g_{n5}^2 - 2\omega_n^2g_{n3}\right)A_n^2\bar{A}_ne^{i\omega_nT_0} + g_{n4}\frac{f}{2}e^{i\Omega T_0} \\ &-\left[g_{n2} + \frac{2}{3}g_{n5}^2 - 2g_{n3}\omega_n^2\right]A_n^3e^{3i\omega_nT_0} \\ &-g_{n1}\left[A_n^2\frac{f}{2}\left(e^{i(2\omega_n+\Omega)T_0} + e^{i(2\omega_n-\Omega)T_0}\right) + A_n\bar{A}_n\frac{f}{2}e^{i\Omega T_0}\right] + cc \end{aligned} \quad (28)$$

The excitation voltage is considered to be a sinusoidal of the form

$$P(t) = \frac{1}{2}fe^{i\Omega t} + cc \quad (29)$$

where f is the voltage magnitude and Ω is the excitation frequency. To describe the nearness of the excitation frequency, Ω, to the natural frequency, ω_n, we introduce the detuning parameter σ, and let

$$\Omega = \omega_n + \varepsilon\sigma\omega_n. \quad (30)$$

Substituting Equation (30) into Equation (28) and eliminating the secular terms and expressing the amplitude in the polar form

$$A_n(T_2) = \frac{1}{2}a_ne^{i\beta_n(T_2)}. \quad (31)$$

then separating the real and imaginary parts of the outcome yields

$$\omega_nD_2a_n = -\frac{1}{2}\hat{\mu}\omega_na_n + \frac{g_{n4}f}{2}\sin\left(\sigma\omega_nT_1 - \beta_n\right), \quad (32)$$

$$\omega_na_nD_2\beta_n = N_{eff}a_n^3 - \left[\frac{g_{n4}f}{2} - \frac{1}{4}g_{n1}fa_n^2\right]\cos\left(\sigma\omega_nT_1 - \beta_n\right). \quad (33)$$

where N_{eff} is a measure of the effective nonlinearity of the system and is given by

$$N_{eff} = \left(3g_{n2} - \frac{10}{3} g_{n5}^2 - 2g_{n3}\omega_n^2\right)/8 . \qquad (34)$$

Eq.(35) shows the steady state condition derived from (32) and (33);

$$\left(\hat{\mu}\omega_n a_n\right)^2 + \left[\frac{N_{eff} a_n^3 - 8\omega_n^2 \sigma a_n}{4 - 2g_{n1} a_n^2} g_{n4}\right]^2 = \left(g_{n4} f\right)^2 \qquad (35)$$

Equation (35) represents the nonlinear *frequency-response* equation for a piezoelectrically-actuated microcantilever sensor. For a given level of voltage excitation f, equation (35) can be solved numerically for the associated response amplitude, a_n. Since g_{n5} appears as a negative and squared term in the effective nonlinearity expression, including the material nonlinearities would certainly decrease the magnitude of the effective nonlinearity of the sensor making the frequency response less and less hardening. For a sensor of known geometry and linear material properties, the coefficients g_{n2} and g_{n3} are well-defined, Table 1. On the other hand, the coefficient g_{n5}, which depends on the nonlinear material properties of the piezoelectric layer, can not be theoretically computed because the experimental value of α_1 is not available in the literature. As such, this coefficient will be obtained experimentally by examining the nonlinear response characteristics of the sensor as illustrated in the next sections.

Table 1. Geometric and Material Properties of the microsensor.

Symbol	Value	Symbol	Value
E_b	185 GPa	E_p	133 GPa
ρ_b	2330 kg/m^3	ρ_p	6390 kg/m
h_b	4 μm	h_p	4 μm
l	500 μm	l_2	375 μm
w_b	250 μm	w_p	130 μm
w_t	55 μm		

5. Experimental Validation

In this section, the experimental setup utilized to validate the nonlinear theoretical model and to identify the unknown linear and nonlinear parameters is presented. The sensor utilized in the experiments is the DMASP® microcantilever beam manufactured by Veeco® Instruments and shown in Fig. 2(right). The beam is actuated by supplying a voltage to a piezoelectric layer made of one 3.5μm Zinc Oxide (ZnO) layer and two 0.25μm Titanium-Gold (Ti/Au) layers. Such microcantilevers have been extensively utilized for scanning and sensing applications. The geometric and material properties of the cantilever are listed in Table 1.

To validate the theoretical model, we compare the frequency-response curves obtained experimentally to those obtained theoretically via equation (35). To that end, two unknown parameters are obtained experimentally. First, the linear damping coefficient $\hat{\mu} = \zeta_{exp}/(2\,\omega_1)$,where ζ_{exp} represents the experimental damping ratio, is obtained using the half-power points approach [20]. For the sensor under consideration, we found that the damping ratio varies between $\zeta_{exp.}$=0.0025 and 0.0034 (air and structural damping). As such we utilized an average value of ζ_{exp}=0.00295.

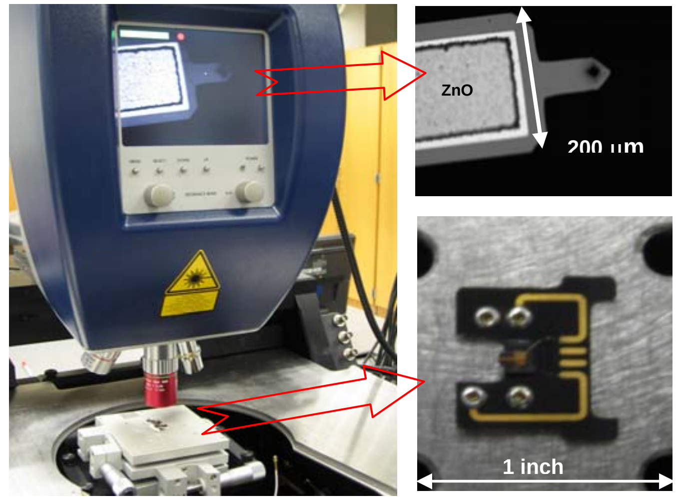

Figure 2. (left) MSA-400 microsystem analyzer, (right) DMASP® microcantilever and microscopic image of microcantilever.

Second, the coefficient of material nonlinearity in the piezoelectric layer is obtained using the frequency-response curves. More specifically, by utilizing the loci of the peaks of the experimental response for different voltages, we curve fit the best quadratic polynomial relating the response peaks to the frequency-detuning parameter. The generated polynomial, known also as the *backbone* curve, is compared to that obtained analytically by finding the extrema of equation (35). These correspond to the solution of

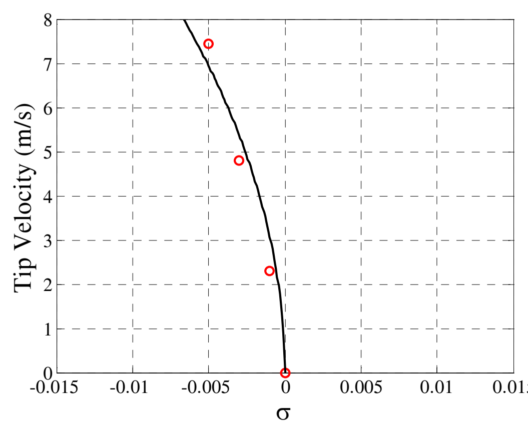

Figure 3. Backbone curve of the frequency response. Circles represent the peaks of the experimentally-obtained frequency response curves and the solid line represents their best quadratic curve fit.

$$a_{1\max} = \sqrt{\frac{8\omega_1^2\sigma}{3g_{12} - 10g_{15}^2/3 - 2g_{13}\omega_1^2}} \qquad (36)$$

The only unknown in Equation (36) is the coefficient g_{15}. By comparing equation (36) to the best polynomial fit shown in Fig. 3, we find that g_{15} is equal to 60 and, hence, by virtue of equation (21g), the material nonlinearity coefficient of the piezoelectric layer can be found to be α_1= 4645.23 GPa.

Using the experimental values of the linear damping and material nonlinearity coefficient, we generate the frequency-response curves via equation (35). These curves are compared to the experimental data in Fig. 4 demonstrating excellent agreement everywhere in the frequency range and not only at the peak frequencies. This clearly illustrates the validity of the proposed model.

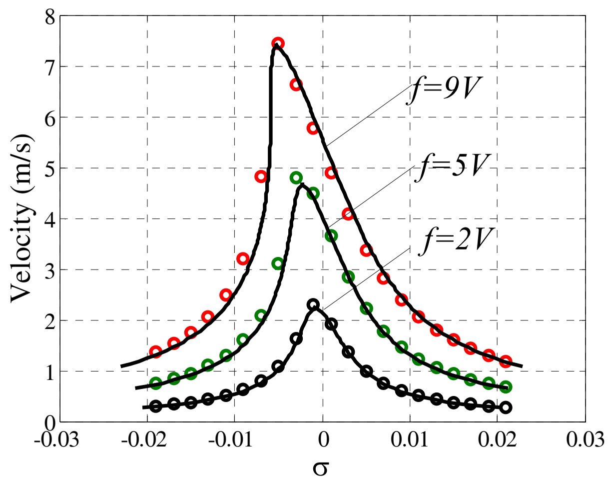

Figure 4. Analytical and experimental frequency response curves. Circles represent experimental data and the solid lines represent analytical results.

6. Conclusions

In order to effectively utilize microcantilever sensors in practice, the chief technical issue related to modeling must be addressed in order to correctly relate the micromechanical response to the adsorbed species. Along this line, the nonlinear equations of motion governing flexural vibrations of these sensors have been derived. The proposed model considered both longitudinal and flexural vibrations of the microcantilever sensor and their coupling in addition to the ever-present nonlinearities due to geometry of the microcantilever. More specifically, it was demonstrated that the electromechanical coupling in these sensors is nonlinear which appeared in quadratic form. Through extensive experimental measurements, the coefficient of such quadratic nonlinear term was determined which compared well with both analytical and experimental results. Finally, the frequency response results clearly demonstrated the presence of nonlinear quadratic term in electromechanical coupling in these sensors.

Acknowledgment

The materials presented here are based upon work supported in part by the National Science Foundation under CAREER Grant No. CMMI-0238987 and MRI program Grant No. CMMI-0619739.

References

[1] Aurelle, N., Guyomar, D., Richard, C., Gonnard, P. and Eyraud L., 1996, "Nonlinear Behavior of an Ultrasonic Transducer", *Ultrasonics*, **34**, 187-191.

[2] Hemsel, T., Mracek, M., Twiefel, J. and Vasijev, P., 2006, "Piezoelectric linear motor concepts based on coupling of longitudinal vibrations", *Ultrasonics*, **44**, e591-e596.

[3] Das, S., Sreeram, P.A., Raychaudhuri, A. K., Sai, T. P. and Brar, L.K., 2006, "Non-Contact Dynamic Mode Atomic Force Microscope: Effects of Nonlinear Atomic Forces", *Proceedings of 2006: IEEE Conference on Emerging Technologies - Nanoelectronics*, 2006, 458-462.

[4] Scherer, V., Arnold, W., Bhushan, B., 1999, "Lateral force microscopy using acoustic friction force microscopy", *Surface and Interface Analysis*, 27(5-6), 578-587.

[5] Yuan, W., Smits, J.G., Dominquez, P., Cantor, C.R. and Smith, C.L., 1998, "Current – Voltage Properties of Piezoelectric Thin Film ZnO in a Micromechanical Force Sensor", *Proceedings of IEEE Ultrasonics Symposium*, **1**, 593-596.

[6] Soderkvist, J., 1992, "Activation and Detection of Mechanical Vibrations in Piezoelectric Beams", *Sensors and Actuators A: Physical*, **32**(1-3), 567-571.

[7] Guyomar, D., Aurelle, N. and Eyraud, L., 1997, "Piezoelectric ceramics nonlinear behavior. Application to Langevin transducer", *Journal De Physique III*, **7**(6), 1197-1208.

[8] Gonnard, P., Perrin, V., Briot, R., Guyomar, D. and Albareda, A., 1998, "Characterization of the piezoelectric ceramic mechanical nonlinear behavior", *Proceedings of IEEE International Symposium on Applications of Ferroelectrics* , 353-356.

[9] Albareda, A., Gonnard, P., Perrin, V., Briot, R., and Guyomar, D. , "Characterization of the mechanical nonlinear behavior of piezoelectric ceramics", *IEEE Transactions on Ultrasonics, Ferroelectrics, and Frequency Control*, **47**(4), 844-853.

[10] Tadmor, E.B., Kosa, G., 2003, "Electromechanical Coupling Correction for Piezoelectric Layered Beams", *Journal of Microelectromechanical Systems*, **12**(6), 899-906.

[11] Lau, C.W.H., Lim, C.W. and Leung, A.Y.T., 2005, "A Variational Energy Approach for Electromechanical Analysis of Thick Piezoelectric Beam", *Journal of Zhejiang University Science*, **6A**(9), 962-966.

[12] Shiah, Y.C., Huang, C. and Huang, J.H., 2006, "Static Electromechanical Response of Piezoelectric Tubes as Sensors and Actuators", *Journal of Intelligent Material Systems and Structures*, **17**, 133-143.

[13] Crespo da Silva, M.R.M. and Glynn, C.C., 1978, "Nonlinear Flexural-Flexural-Torsional Dynamics of Inextensional Beams: I. Equations of Motion", *Journal of Structural Mechanics*, **6**(4), 437-448.

[14] Crespo da Silva, M.R.M. and Glynn, C.C., 1978, "Nonlinear Flexural-Flexural-Torsional Dynamics of Inextensional Beams: II. Forced Motions", *Journal of Structural Mechanics*, **6**(4), 449-461.

[15] Dadfarnia, M., Jalili, N., Xian, B., and Dawson, D. M., 2004, "A Lyapunov-Based Piezoelectric Controller for Flexible Cartesian Robot Manipulators", *ASME Journal of Dynamic Systems, Measurement, and Control*, **126**, 347-358.

[16] Dadfarnia, M., Jalili, N., Liu, Z., and Dawson, D. M., 2004, "An Observer-based Piezoelectric Control of Flexible Cartesian Robot Arms: Theory and Experiment" *Control Engineering Practice*, **12**, 1041–1053.

[17] Mahmoodi, S.N. and Jalili, N., 2007, "Non-linear vibrations and frequency response analysis of piezoelectrically driven microcantilevers", International *Journal of Non-Linear Mechanics*, **42**, 577 – 587.

[18] Mahmoodi, S.N., and Jalili, 2006, "An Experimental and Theoretical investigation on Nonlinear Vibrations of Piezoelectrically-driven Microcantilevers", *Proceedings of 2006 ASME International Mechanical Engineering Congress & Exposition,* Symp. on Vibration and Noise Control, Chicago, IL (November 2006).

[19] Mahmoodi, S.N. and Jalili, N., 2007, "Coupled Flexural-Torsional Nonlinear Vibrations of Microcantilever Beams", *Proceedings of the 14th International SPIE 2007 Smart Structures & Materials Conference*, San Diego, CA (February 2007).

[20] Meirovitch, L., *Analytical Methods in Vibrations*, Prentice Hall, 1997.

[21] Nayfeh, A. H., *Perturbation Methods*, Wiley, 1973.